Structural Profile of Ultra-High Molecular Weight Polyethylene in Acetabular Cups Worn on Hip Simulators Characterized by Confocal Raman Spectroscopy

Leonardo Puppulin,[1] Tsuyoshi Kumakura,[1,2] Kengo Yamamoto,[2] Giuseppe Pezzotti[1]

[1]Kyoto Institute of Technology, Ceramic Physics Laboratory & Research Institute for Nanoscience, RIN, Sakyo-ku, Matsugasaki, 606-8585 Kyoto, Japan, [2]Department of Orthopaedic Surgery, Tokyo Medical University, Shinjuku-ku, 6-7-1 Nishishinjuku, 160-0023 Tokyo, Japan

Received 9 April 2010; accepted 15 November 2010
Published online 18 January 2011 in Wiley Online Library (wileyonlinelibrary.com). DOI 10.1002/jor.21331

ABSTRACT: We applied a Raman confocal spectroscopic technique to quantitatively assess the structural features of two kinds of acetabular cups made of ultra-high molecular weight polyethylene. We wanted to know whether polyethylene cups belonging to different generations, and thus manufactured by different procedures, possess different molecular structures and how those differences affected their wear resistance. Emphasis was placed on oxidation profiles developed along the cross-sectional depth of the cups in the main wear zone developed during testing in a hip simulator. The micrometric lateral resolution of the laser beam, focused at surface or sub-surface sectional planes, enabled the visualization of highly resolved microstructural property profiles, including crystalline and amorphous phase fractions. Oxidation profiles retrieved from polyethylene cups belonging to different generations greatly differed after wear testing. The highly cross-linked polyethylene showed a lower degree of crystallinity and oxidation at an appreciably slower rate as compared to that belonging to an earlier generation. © 2011 Orthopaedic Research Society. Published by Wiley Periodicals, Inc. J Orthop Res 29:893–899, 2011

Keywords: acetabular cup; UHMWPE; hip simulator; Raman spectroscopy; wear rate; oxidation

Formation of ultra-high molecular weight polyethylene (UHMWPE) wear debris represents the most critical concern in long-term implanted total hip replacements (THR) and has been reported as the most serious cause of implant failure (i.e., because debris particles can cause osteolysis[1,2] and prosthesis loosening[3,4]). To minimize polyethylene wear, gamma irradiation is currently used as a sterilization procedure.[5] Gamma irradiation generates free radicals through homolytic bond cleavage, which leads to cross-linking and chain scission. Conversely, oxidation can partly occur to produce a major change in the irradiated polyethylene structure in the presence of oxygen.[6] This phenomenon leads to enhanced wear and reduced mechanical properties, unraveling the positive effect of gamma-ray irradiation.[7] Early polyethylenes were manufactured with a melting or annealing step to quench free radicals. Molten polyethylene exhibits significantly altered crystallinity, which results in a marked reduction of mechanical strength[8–10] with cracking, pitting, and catastrophic fracture reported clinically.[11,12] Conversely, annealed polyethylene exhibits high mechanical strength, but can trap a significant amount of free radicals, which can in turn greatly increase the oxidation potential of the material. Left untreated, a high level of free radicals can thus form in the annealed polyethylene.[13,14] A second-generation polyethylene is being developed that maintains high wear resistance but preserves mechanical strength and avoids oxidation by solid-state deformation (e.g., ArComXL™ polyethylene) or antioxidant diffusion of vitamin E.[15] In vitro testing produced compelling results for many highly cross-linked polyethylene materials, but skeptics counter that similarly encouraging data were produced with discontinued polyethylenes, like Hylamer®, Heat-Pressed Polyethylene, and Poly II® materials.

We suggested[16,17] the use of Raman spectroscopy to nondestructively characterize the oxidation state of biomedical polyethylene grades. Raman spectroscopy was previously used to characterize the degree of crystallinity and the amounts of orthorhombic and amorphous phases.[18–22] Raman characterization in the backscattered configuration can be conducted on bulk samples nondestructively. Furthermore, using the confocal Raman probe,[16] one might screen the polyethylene structure in the depth of the liner without sectioning.

Thus, we compared acetabular cups made of two types of polyethylenes, the old ArCom® and new ArComXL™. We compared their microstructures and how they evolved during wear testing, evaluating degree of crystallinity, amorphous phase fraction, and oxidation index profiles along the subsurface. We believe the Raman microprobe is a fast, high resolution, minimally intrusive tool for characterizing polyethylenes.

MATERIALS AND METHODS

Materials

Two types of acetabular cups were examined, which were both manufactured by Biomet Inc., Warsaw, IN. The total number of samples was 36. The materials were obtained from the same resin and manufactured by isostatic compression molding, but they differed in irradiation dose, post-radiation treatment, and sterilization method (Table 1). ArCom® components were cleaned, vacuum-sealed with an argon purge, and gamma sterilized with a dose between 25 and 40 kGy. ArComXL™ components were stress relieved, gamma-irradiated with 50 kGy dose, and processed through a solid-state deformation process

Correspondence to: Giuseppe Pezzotti (T: 81-75-724-7568; F: 81-75-724-7568. E-mail: pezzotti@kit.ac.jp)

Table 1. Manufacturing Characteristics of the Two Types of Polyethylene

	Resin	Processing Method	γ-Ray Dose (kGy)	Post-Radiation Treatment	Sterilization Method
ArCom®	GUR1050	Isostatically compression molded	25–40	None	Gamma in argon
ArComXL™	GUR1050	Isostatically compression molded	50	Solid-state deformation	Gas plasma

to increase oxidation resistance. They were cleaned, packaged in a tyvex pouch, and sterilized by gas plasma.

Hip Simulator Wear Testing

Wear tests were carried out in an 8-channel hip simulator (Biomet) against the same type of CoCr metallic head. The liners were press fitted into a stainless steel holder. The modular heads were mounted onto Ti-6A1-4V taper adapters that were connected to the self-centering mount on the simulator. The simulator applied an anatomical load profile (Paul hip curve) with a 2.0 kN maximum load, 1.0 Hz frequency, and 23° biaxial oscillation at room temperature.[23] Each sample was characterized in its as-received state and after different wear duration times (0.1, 0.5, 1.0, 3.0, and 5.0 million cycles). Bovine calf serum was used as a lubricant (New Born Calf Serum, 2:1 dilution with water; JRH, Biosciences, Lenexa, KS). After each time period, the cups were removed, and mass loss data were collected. The volumetric loss (mm^3) was calculated dividing the mass by the density (0.993 g/cm^3). Then all the cups were vacuum-sealed and delivered to the Raman spectroscopy laboratory.

Confocal Raman Spectroscopy

Raman spectra were collected with an optical microprobe and analyzed by a single monochromator spectrometer (T-64000, ISA Jovin-Ivon/Horiba Group, Tokyo, Japan) equipped with a charge-coupled detector. The laser excitation frequency was 488 nm, spectral integration time was typically 20 s, with spectra averaged over three successive measurements at each selected location. The samples were scanned using an automatic mapping device along their in-plane x and y axes. A standard range for the Raman maps was a square area of 50 μm on which 12 × 12 points were collected per map (a measurement time of about 2 h 20 min per map). Locations were selected in the main wear zone (10° from the polar cup axis, Fig. 1). To minimize *in-depth* convolution of the Raman spectra, a confocal pinhole was used. In this way, the probe size could be confined to 2.2 and 6.4 μm in plane and in depth, respectively. Details of confocal probe deconvolution procedures were previously reported.[16] Measurement depths, z_0, of the focal plane of the Raman probe were selected at 0, 5, 10, 20, 30, 40, and 50 μm (Fig. 1). At each depth, 2D Raman maps were collected for each acetabular component.

The spectroscopic correlations between Raman bands and microstructural features of polyethylene are available[18–22] (Table 2). Figure 2 shows a typical spectrum after deconvolution performed by a commercially available automatic fitting algorithm (Labspec 3, Horiba/Jobin-Yvon, Kyoto, Japan) using mixed Gaussian/Lorentzian curves. The spectrum (shown here between 950 and 1,600 cm^{-1}) can be divided into three regions:

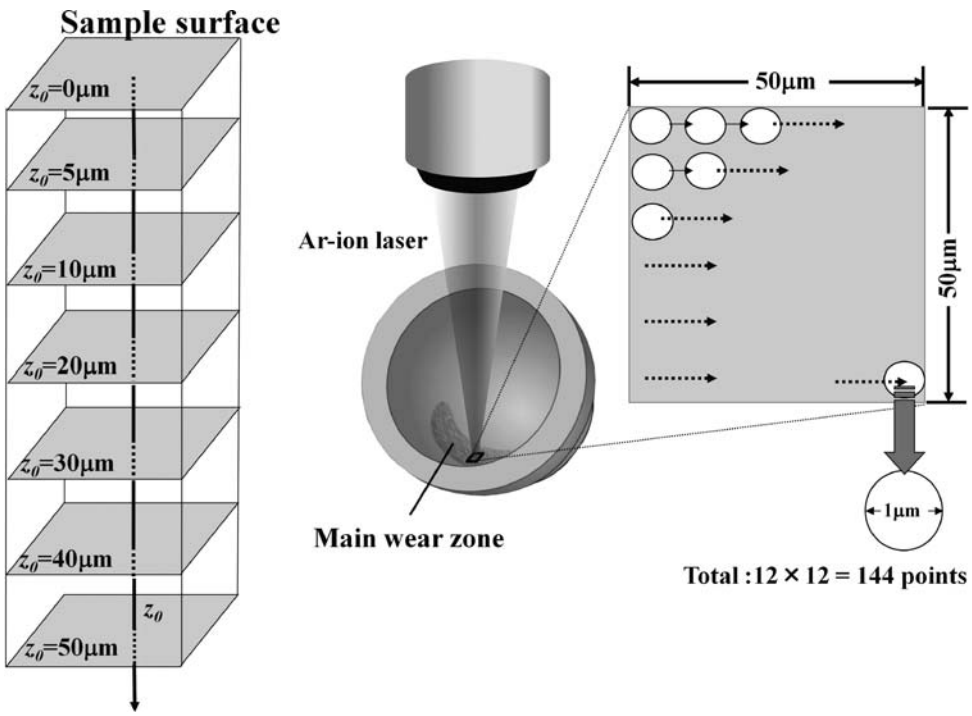

Figure 1. The procedure used to collect Raman spectra from the hip cups. The map size was 50 μm × 50 μm, and the square mesh was characterized by about 4.5 μm steps.

Table 2. Raman Bands and Respective Vibrational Modes in Polyethelene

Wave Number (cm^{-1})	Mode	Phase
Region I		
1,060	$\upsilon_{as}CC$	Crystalline + trans
1,080	υCC	Amorphous
1,127	$\upsilon_{s}CC$	Crystalline + trans
Region II		
1,293	τCH_2	Crystalline
1,305	τCH_2	Amorphous
Region III		
1,414	δCH_2	Crystalline
1,440	δCH_2	Amorphous + trans
1,460	CH_2	Amorphous

Spectral locations (wave number, cm^{-1}) are indicated together with the related phases, vibrational modes, and symmetries. υ, stretching; υ_{as}, asymmetric stretching; υ_s, symmetric stretching; τ, twisting; δ, bending.

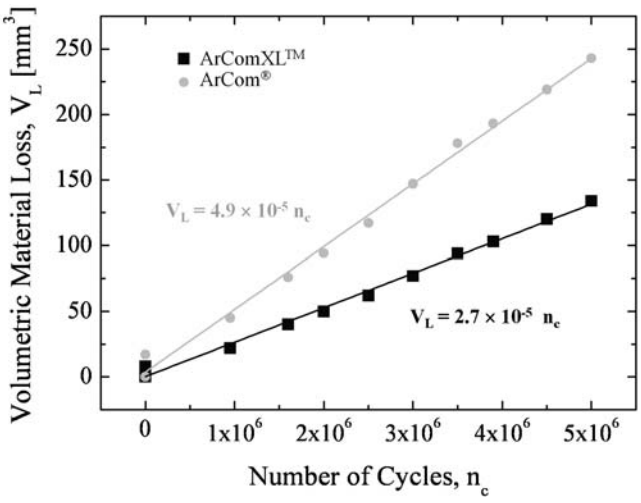

Figure 3. Profiles of wear rate results as a function of testing time in the hip simulator for both UHMWPE cups (ArCom® cups and ArComXL™ cups). Data scatter is represented by the size of the respective symbols.

region I, dominated by the C–C stretching vibrational mode in the interval 1,000–1,150 cm^{-1}; *region II*, represented by the $-CH_2-$ twisting vibration at ~1,300 cm^{-1}; and *region III* characteristic of $-CH_2-$ bending between 1,350 and 1,500 cm^{-1}. The broad band at 1,080 cm^{-1} is associated with the presence of an amorphous phase.[20] The peak at 1,414 cm^{-1} is characteristic of an orthorhombic phase, representing the crystalline phase; the peak at 1,293 cm^{-1} can be used to approximate the degree of crystallinity in the overall structure.[18–22] The percentages of crystalline (α_c) and amorphous (α_a) phases can be calculated from the Raman spectrum according to the following equations[20]:

$$\alpha_c = \frac{I_{1293}}{I_{1293} + I_{1305}} \times 100 \quad (1)$$

$$\alpha_a = \frac{I_{1080}}{0.79(I_{1293} + I_{1305})} \times 100 \quad (2)$$

where I is the integral intensity of each band after deconvolution.

Raman and FTIR spectroscopic characterizations were previously performed on a series of UHMWPE oxidized samples.[16] Validation of a relationship between oxidation index (OI), and selected bands in *regions II* and *III* were:

$$OI = \exp\left\{1.19 \times \tan\left[14.26\left(\frac{I_{1414}}{I_{1293} + I_{1305}} - 0.26\right)\right] - 0.13\right\} \quad (3)$$

Three cups were used for each wear duration time and each polyethylene. Results were consistent within a group, so averages and standard deviations for each time were calculated:

$$\overline{a} = \frac{\sum_{i=1}^{3N} a_i}{3N} \quad (4)$$

$$\Delta a = \sum_{i=1}^{3N} \sqrt{\frac{(a_i - \overline{a})^2}{3N}} \quad (5)$$

where $a = \alpha_c$, α_a or OI and $N = 144$ is the number of points collected for each map.

RESULTS

The wear rate of the ArComXL™ was improved compared to ArCom® (Fig. 3). These data support previously published data.[24,25] For the as-received state up to a wear duration of 3 M cycles, the crystallinity fractions in the ArCom® cups were comprised within a narrow range of 45–50%, approximately the same at depths $\geq$10 μm (Fig. 4). The degree of crystallinity increased to $\geq$50% after 5 M cycles, showing a less abrupt increase along the *in-depth* abscissa between 0 and 10 μm as compared to cups analyzed between 0 and

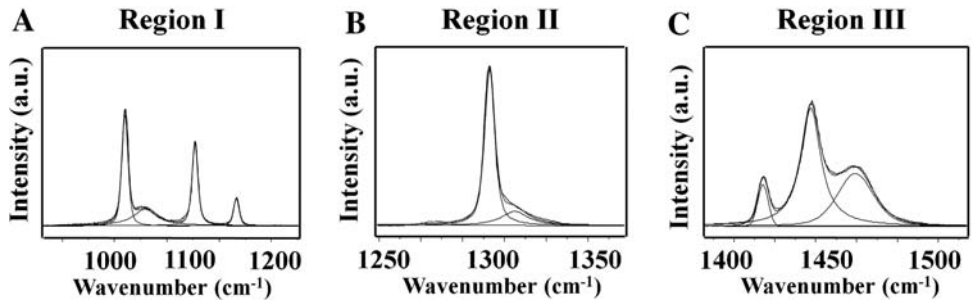

Figure 2. Typical Raman spectrum of PE. Spectral deconvolution into Gaussian/Lorentzian sub-bands is also shown as performed by an automatic computational routine.

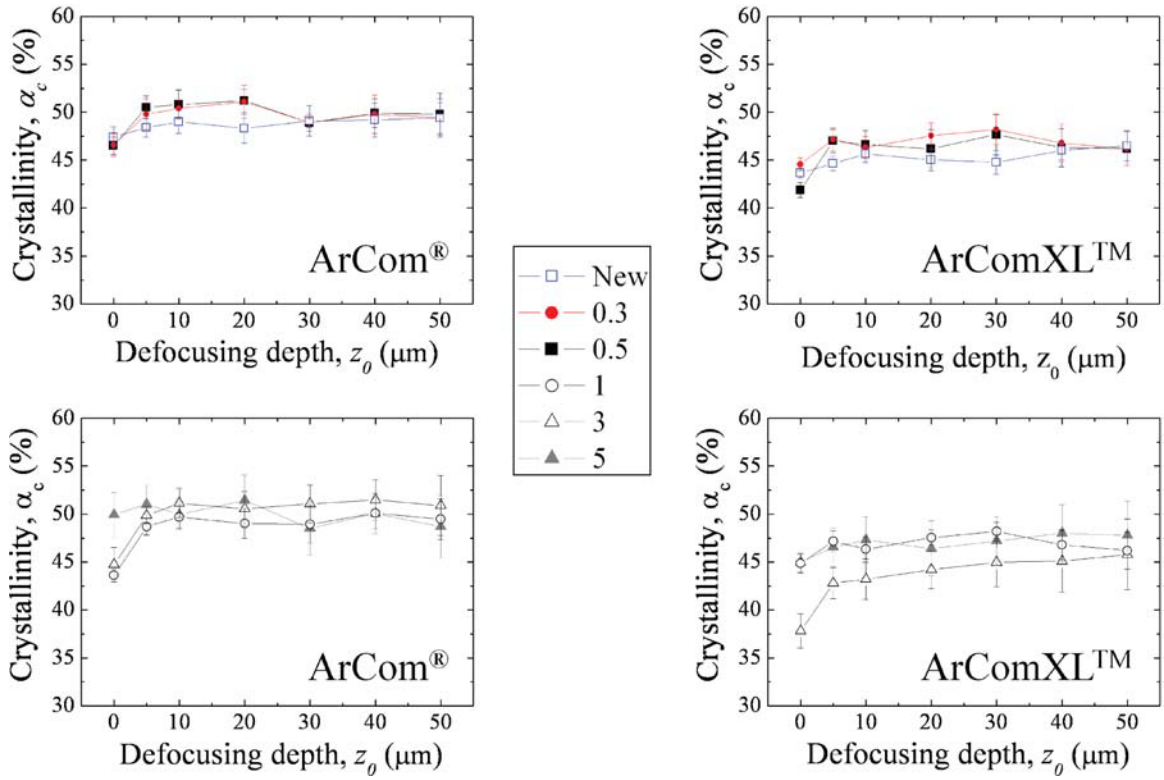

Figure 4. Crystalline phase fraction profiles as calculated from ArCom® and ArComXL™ cups (as per Equation 1). Symbols represent testing duration in the simulator (million of cycles).

3 M cycles. A similar trend was found for the ArComXL™ cups although the maximum increase in crystallinity fraction between surface and sub-surface was within a lower range of 40–49%. The fractions of amorphous phase in the ArCom® cups decreased from a range of 50–55% to a minimum at ~43% at a depth of about 20 μm, and then mildly increased again up to about 47% at depths of 50 μm (Fig. 5). The amorphous fractions in the ArComXL™ cups showed a similar trend, but were within a higher range between ~55% on the surface (though at 3 M cycles a slightly higher value was measured) and 52% at a depth of 50 μm, with a minimum of ~47% at a depth of 20 μm. Adding amorphous and crystalline fractions does not yield 100% because of the presence of a minor fraction of an intermediate phase.[26]

The OI values in the ArComXL™ cups were low (Fig. 6) and increased only slightly with increasing sub-surface depth. ArCom® cups revealed a larger increase in OI in the immediate subsurface at around 10 μm. This increase was noticed in all ArComXL™ cups tested in the simulator, but not in the as-received cups. Oxidation profiles seem to demonstrate a tangible improvement in structural stability for ArComXL™ as compared to ArCom® cups.

DISCUSSION

We found that the higher crystalline fraction found in ArCom® corresponded to a more pronounced oxidative behavior (Figs. 4 and 6) as compared to ArComXL™. This difference can be attributed to a larger population of free radicals in the former cups. Furthermore, enhanced crystallization often accompanies enhanced oxidation during in vivo exposure.[27] Thus, our wear study might support in vivo data. Moreover, Shen and McKellop[28] recently showed that irradiation in the presence of residual oxygen in the atmosphere induces oxidation instead of crosslinking, so that the level of crosslinking achieved is lower than that which would normally occur at the same dose in the absence of oxygen. The formation of an oxidation peak below the free surface is due to the combined effects of the distribution of residual-free radicals and the oxygen diffusion gradient. This suggests that the higher oxidation resistance and significantly lowered wear rate of ArComXL™ arise from better control during manufacturing with lower crystallization in an absence of oxygen at higher gamma irradiation doses.

Nevertheless, the OI was always well below 3, which is associated with a "critical" step in the loss in mechanical properties and with a propensity for fatigue damage in vivo.[29] Thus, OI < 1 is an insignificant level of oxidation and, not affecting the ultimate mechanical strength, but only the wear lifetime with respect to degradation. Accurate Raman studies require a cumbersome characterization in terms of number of spectra to be collected at different locations. This circumstance, which led us to follow the tribological evolution of a limited number of

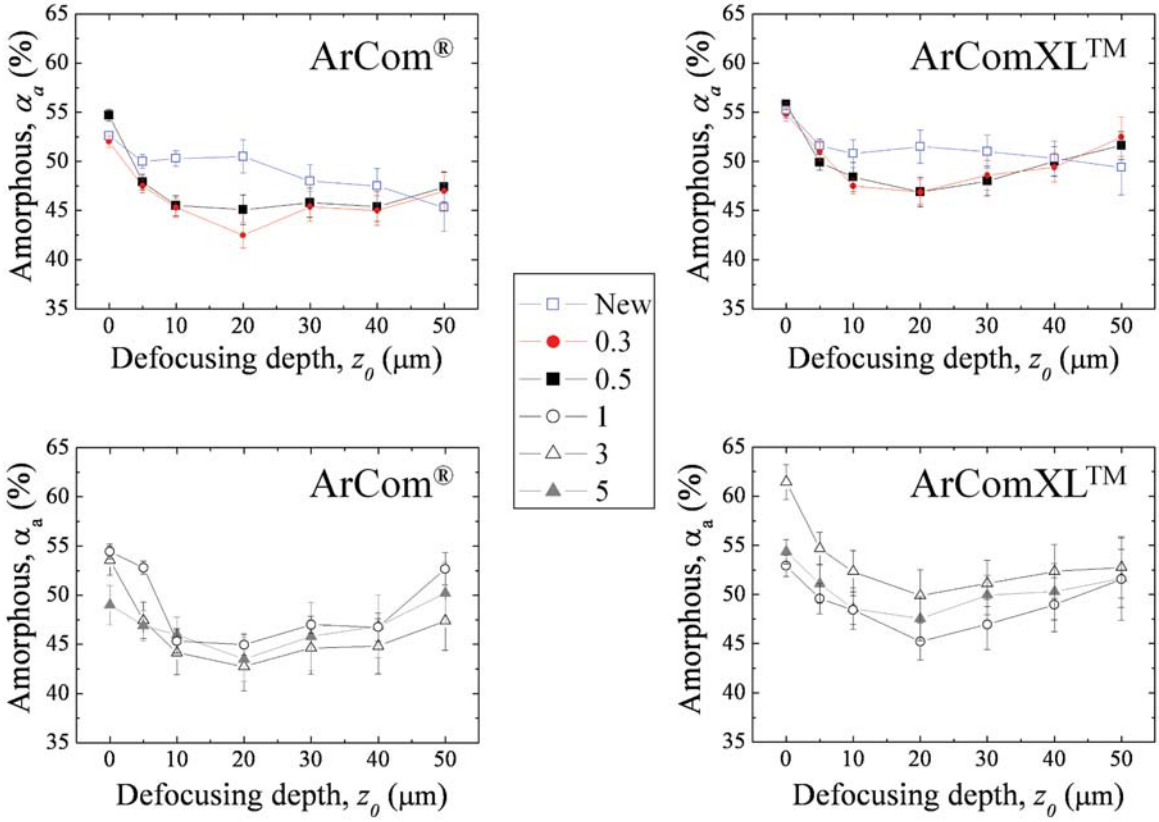

Figure 5. Amorphous phase fraction profiles as calculated from ArCom® and ArComXL™ cups (as per Equation 2). Symbols represent testing duration in the simulator (million of cycles).

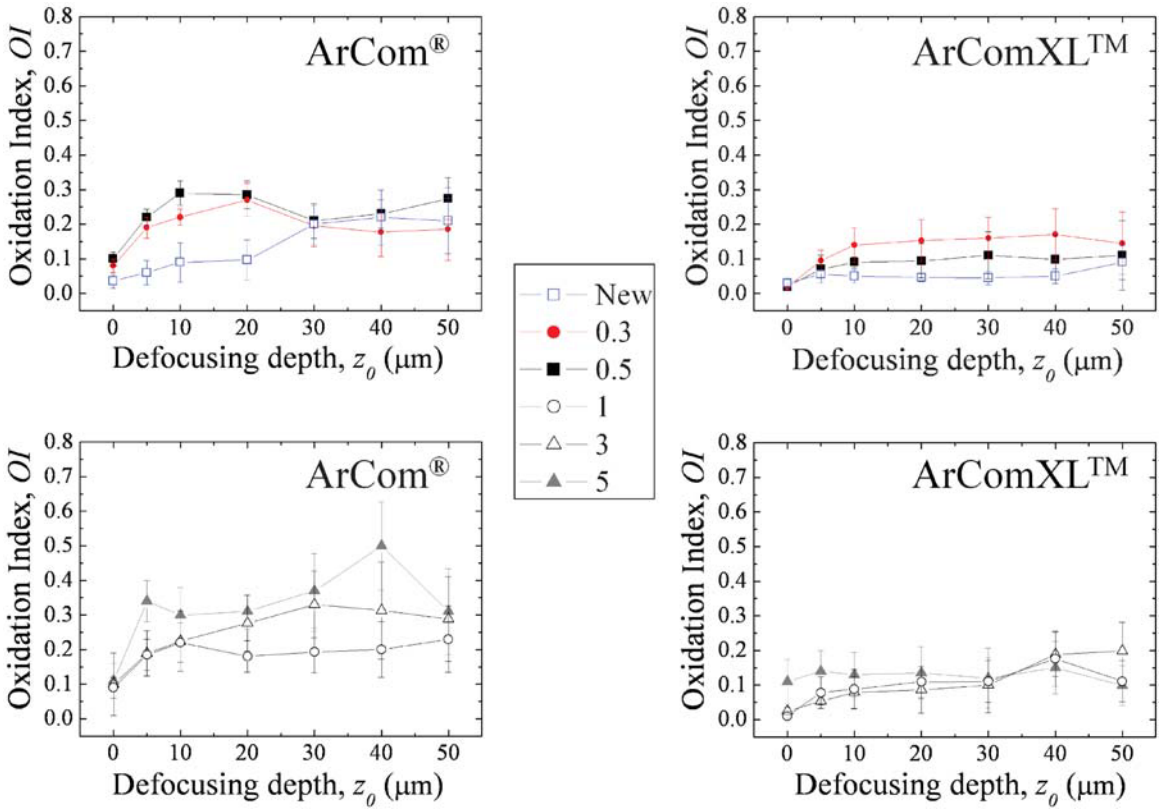

Figure 6. Profiles of OI as calculated from ArCom® and ArComXL™ cups as per Equation (3). Symbols represent testing duration in the simulator (million of cycles).

cups, places an upper limit to the number of samples that can be examined in a reasonable time. Another limitation of our study is the unavailability of retrievals, which would allow comparison between the in vivo performances of the two polyethylene types. However, we believe that the Raman study on specimens after long-term wear testing reveals the salient structural characteristics on the molecular scale.

In summary, confocal microprobe Raman spectroscopy was applied to characterize nondestructively and with high-spatial resolution *in-depth* structural characteristics of polyethylene acetabular cups. The results clarify the difference in physicochemical conditions of hip cups belonging to different generations on their surface after in vitro simulation, and show the suitability of confocal Raman spectroscopy for systematic studies of UHMWPE components, revealing near-surface characteristics for the first time. Moreover, the actual oxidation state of polyethylene liners in the neighborhood of the irradiated surface is difficult to characterize with high-spatial resolution, which in turn leads to a lack of direct experimental evidence on the impact of different processing steps. In experimental practice, the degree of oxidation is usually measured by infrared spectroscopy,[30–32] but unfortunately this measurement is destructive in nature, which might involve alterations in the oxidation state of the sample, makes measurement of oxidation profiles quite time consuming, and limits the achievable spatial resolution.

ACKNOWLEDGMENTS

No commercial funds were received. Samples were kindly supplied by Tokyo Medical University.

REFERENCES

1. Zhu YH, Chiu KY, Tang WM. 2001. Polyethylene wear and osteolysis in total hip replacement. J Orthop Surg 9:91–99.
2. Oparaugo PC, Clarke IC, Malchau H, et al. 2001. Correlation of wear debris-induced osteolysis revision with volumetric wear rates of polyethylene. Acta Orthop Scand 72:22–28.
3. Amstutz HC, Campbell P, Kossovsky N, et al. 1992. Mechanisms and clinical significance of wear debris-induced osteolysis. Clin Orthop 276:7–18.
4. Clarke IC, Campbell P, Kossowsky N. 1992. Debris-mediated osteolysis: a cascade phenomenon involving motion, wear, particulates, macrophage induction and bone lysis. In: St. John. SE editor. Particulate debris from medical implants: mechanisms of formation and biological consequences. Philadelphia: American Society for Testing and Materials; p 7–26.
5. Bargmann LS, Bargmann BC, Collier JP, et al. 1999. Current sterilization and packaging methods for polyethylene. Clin Orthop 369:49–58.
6. Yeom B, Yu Y-J, McKellop HA, et al. 1998. Profile of oxidation in irradiated polyethylene. J Polym Sci A Polym Chem 36:329–339.
7. Goldman M, Gronsky R, Long GG, et al. 1998. The effects of hydrogen peroxide and sterilization on the structure of ultra high molecular weight polyethylene. Polym Degrad Stabil 62:97–104.
8. Baker DA, Bellare A, Pruitt L. 2003. The effects of degree of crosslinking on the fatigue crack initiation and propagation resistance of orthopedic-grade polyethylene. J Biomed Mater Res 66A:146–154.
9. Gomoll A, Wanich T, Bellare A, et al. 2001. Quantitative measurement of the morphology and fracture toughness of radiation cross-linked UHMWPE. 47th Annual Meeting, Orthopaedic Research Society, San Francisco.
10. Gillis A, Schiemg JJ, Bhattacharyya S, et al. 1999. An independent evaluation of the mechanical, and fracture properties of UHMWPE cross-linked by 34 different conditions. 45th Annual Meeting, Orthopaedic Research Society, Anaheim.
11. Bradford L, Baker DA, Graham J, et al. 2004. Wear and surface cracking in early retrieved highly cross-linked polyethylene acetabular liners. J Bone Joint Surg 86A:1271–1282.
12. Halley D, Glassman A, Crowninshield RD, et al. 2004. Recurrent dislocation after revision total hip replacement with a large prosthetic femoral head. J Bone Joint Surg 86A:827–830.
13. Bhattacharyya S, Doherty AM, Wannomae KK, et al. 2004. Severe in vivo oxidation in a limited series of retrieved highly crosslinked UHMWPE acetabular components with residual free radicals. Orthopaedic Res Soc No. 0276. Proceedings 55th annual meeting orthopaed Res. Soc., Las Vegas.
14. Muratoglu O, Merrill EW, Bragdon R, et al. 2004. Effect of radiation, heat, and aging on in-vitro wear resistance of polyethylene. Clin Ortho Relat R 417:253–262.
15. Oral E, Wannomae KK, Hawkins N, et al. 2004. Alpha-tocopherol-doped irradiated UHMWPE for high fatigue resistance and low wear. Biomaterials 25:5515–5522.
16. Pezzotti G, Kumakura T, Yamada K, et al. 2007. Confocal Raman spectroscopic analysis of cross-linked ultra-high molecular weight polyethylene for application in artificial hip joints. J Biomed Opt 12:014011–014014.
17. Kumakura T, Puppulin L, Yamamoto K, et al. 2009. In-depth oxidation and strain profiles in UHMWPE acetabular cups non-destructively studied by confocal Raman microprobe spectroscopy. J Biomater Sci Polym Ed 20:1809–1822.
18. Taddei P, Affatato S, Fagnano C, et al. 2002. Vibrational spectroscopy of ultra-high molecular weight polyethylene hip prostheses: influence of the sterilization method on crystallinity and surface oxidation. J Mol Struct 613:121–129.
19. Mutter R, Stille W, Strobl GR. 1993. Transition regions and surface melting in partially crystalline polyethylene: a Raman spectroscopic study. J Polym Sci B Polym Phys 31:99–105.
20. Strobl GR, Hagedorn W. 1978. Raman spectroscopic method for determining the crystallinity of polyethylene. J Polym Sci Polym Phys Ed 16:1181–1193.
21. Rull F, Prieto AC, Casado JM, et al. 1993. Estimation of crystallinity in polyethylene by Raman spectroscopy. J Raman Spectr 24:545–550.
22. Glotin M, Mandelkern L. 1982. A Raman spectroscopic study of the morphological structure of the polyethylenes. Colloid Polym Sci 260:182.
23. Paul JP. 1967. Forces transmitted by joints in the human body. Proc Inst Mech Eng 181:8–15.
24. Galvin AL, Tipper JL, Jennings LM, et al. 2007. Wear and biological activity of highly crosslinked polyethylene in the hip under low serum protein concentrations. Proc Inst Mech Eng H 221:1–10.
25. Rothman RH. 2007. The bearing of the future. Delta ceramics vs highly crosslinked polyethylene. Proceeding in 12th International BIOLOX Symposium.
26. Nylor CC, Meier RJ, Kip BJ, et al. 1995. Raman spectroscopy employed for the determination of the intermediate phase in polyethylene. Macromolecules 28:2969–2978.
27. Puolakka TJS, Keranen JT, Juhola KA, et al. 2003. Increased volumetric wear of polyethylene liners with more than 3 years of shelf-life time. Int Orthopaed 27:153–159.

28. Shen FW, McKellop HA. 2002. Interaction of oxidation and crosslinking in gamma-irradiated ultrahigh molecular-weight polyethylene. J Biomed Mater Res 61:430–439.
29. Hood RW, Wright TM, Burstein AH. 1983. Retrieval analysis of total knee prostheses: a method and its application to 48 total condylar prostheses. J Biomed Mater Res 17:829–842.
30. Chenery DH. 1997. Detection of peroxy species in ultra-high-molecular-weight polyethylene by Raman spectroscopy. Biomaterials 18:415–419.
31. Goldman M, Lee M, Gronsky R, et al. 1997. Oxidation of ultra high molecular weight polyethylene characterized by Fourier Transform Infrared Spectrometry. J Biomed Mater Res 37: 43–50.
32. Kurtz SM, Muratoglu OK, Buchanan FJ, et al. 2001. Interlaboratory studies to determine optimal analytical methods for measuring the oxidation index of UHMWPE. Biomaterials 22:2875–2881.